Symmetry of Orbital Order in Fe_3O_4 Studied by Fe $L_{2,3}$ Resonant X-Ray Diffraction

A. Tanaka,[1] C. F. Chang,[2,3] M. Buchholz,[2] C. Trabant,[2,4] E. Schierle,[4] J. Schlappa,[2,4] D. Schmitz,[4] H. Ott,[2] P. Metcalf,[5] L. H. Tjeng,[2,3] and C. Schüßler-Langeheine[2,4]

[1]*Department of Quantum Matters, ADSM, Hiroshima University, Higashi-Hiroshima 739-8530, Japan*
[2]*II. Physikalisches Institut, Universität zu Köln, Zülpicher Straße 77, 50937 Köln, Germany*
[3]*Max Planck Institute CPfS, Nöthnizer Straße 40, 01187 Dresden, Germany*
[4]*Helmholtz-Zentrum Berlin für Materialien und Energie GmbH, Albert-Einstein-Straße 15, 12489 Berlin, Germany*
[5]*Department of Chemistry, Purdue University, West Lafayette, Indiana 47907, USA*

(Received 7 August 2011; published 30 May 2012)

We studied the symmetry of the Fe $3d$ wave function in magnetite below the Verwey temperature T_V with resonant soft-x-ray diffraction. Although the lattice structure of the low-temperature phase of Fe_3O_4 is well described by the pseudo-orthorhombic $Pmca$ with a slight monoclinic $P2/c$ distortion, we find that the $3d$ wave function does not reflect the $Pmca$ symmetry, and its distortion toward monoclinic symmetry is by far larger than that of the lattice. The result supports a scenario in which the Verwey transition involves the ordering of t_{2g} orbitals with complex-number coefficients.

DOI: 10.1103/PhysRevLett.108.227203 PACS numbers: 75.25.Dk, 61.05.C−, 61.50.−f, 71.30.+h

Already known as lodestone in ancient Greece, magnetite (Fe_3O_4) has long attracted attention as a magnetic material. Nowadays, it is shown to be a ferrimagnet below $T_N \sim 860$ K. The interest in this material has been rekindled by Verwey's 1939 discovery of a mysterious transition [1], where resistivity increases abruptly by 2 orders of magnitude at $T_V \sim 120$ K [2].

The Verwey transition accompanies a structural phase transition from the cubic inverse spinel to a distorted structure. The lattice symmetry of the low-temperature phase is thought to be monoclinic [3,4] Cc or triclinic [5,6] $P1$ with a $\sqrt{2}a_c \times \sqrt{2}a_c \times 2a_c$ supercell (a_c is the cubic lattice parameter). Recently, Wright *et al.* have refined the crystal structure using x-ray and neutron powder diffraction data, assuming an $a_c/\sqrt{2} \times a_c/\sqrt{2} \times 2a_c$ subcell with $P2/c$ symmetry under pseudo-orthorhombic $Pmca$ symmetry constraints as an approximated structure model [7,8]. Despite the remaining controversy about the symmetry at the low temperatures, the distortion from the Cc monoclinic cell is commonly accepted to be very small [9].

More controversial is the mechanism of the Verwey transition. Different kinds of ordering below T_V in minority-spin t_{2g} orbitals of Fe ions on octahedrally coordinated B sites ($Fe^{2.5+}$ with $t_{2g\uparrow}^3 e_{g\uparrow}^2 t_{2g\downarrow}^{0.5}$ configuration in average) have been proposed to explain the transition: charge ordering [10–12], orbital ordering [13,14], and bond dimerization caused by the Peierls instability [15]. A t_{2g}-orbital and charge order has recently been predicted by band-structure theory with local density approximation with Hubbard U (LDA + U) methods [16–19] using the lattice structure data of Wright *et al.* as input. In addition to this real-number orbital-charge ordered (ROO-CO) state, a theory with complex-number orbital-ordered (COO) state has been proposed [20], where ordered orbitals are described by linear combinations of $|yz\rangle$, $|zx\rangle$, and $|xy\rangle$ wave functions with complex-number coefficients.

The t_{2g}-orbital order has been recently studied using resonant soft-x-ray diffraction (RSXD) from the $(00\frac{1}{2})_c$ superstructure (notation refers to the cubic room-temperature unit cell) at the O $1s \rightarrow 2p$ (K) (Ref. [21]) and Fe $2p \rightarrow 3d$ ($L_{2,3}$) (Ref. [22]) resonances. The $(00\frac{1}{2})_c$ at O K resonance was interpreted by Huang *et al.* as a signature of a particular charge or orbital order at the oxygen sites [21]. At the Fe $L_{2,3}$ edges, the $(00\frac{1}{2})_c$ maximum energy coincides with the resonance of the $2+$ B-site ions and was assigned by Schlappa *et al.* to Fe t_{2g}-orbital order [22]. These interpretations of the origin of the $(00\frac{1}{2})_c$ superstructure, however, have been challenged and an interpretation of $(00\frac{1}{2})_c$ as dominated by lattice distortions and not orbital order was put forward instead [23–25].

To identify a possible orbital order below T_V, it is crucial to detect directly the space group symmetry of the $3d$ electronic state. Resonant soft-x-ray diffraction at the transition-metal $L_{2,3}$ edge involves a $2p \rightarrow 3d$ dipole excitation and is therefore particularly sensitive to the $3d$ electronic state [26–29]. In order to determine the symmetry of the $3d$ electronic state, we studied the azimuth angle and polarization dependence of the $(00\frac{1}{2})_c$ reflection. In this Letter, we show that the space-group symmetry of the $3d$ state below T_V deviates much stronger toward monoclinic than that to be expected from the pseudo-orthorhombic $Pmca$ lattice structure. Consequently, an interpretation of the RSXD data in terms of lattice distortion effects can be ruled out, and our results directly verify that the $(00\frac{1}{2})_c$ superstructure has its origin in orbital order. Furthermore, the ROO-CO state predicted by band-structure theory, which inherits the $P\underline{mc}a$ symmetry of the lattice, is not compatible with our finding that the $3d$

state is much more distorted toward monoclinic symmetry than the lattice.

The soft x-ray scattering experiments were performed at beam lines UE52-SGM and UE46-PGM-1 of the electron storage ring BESSY II operated by the Helmholtz-Zentrum Berlin. The experimental setup is the same as described in Refs. [22,30]. The polarization of incoming light was either perpendicular (σ polarization) or parallel (π polarization) to the diffraction plane. For the azimuth-dependent study of the scattering intensity, the sample was rotated around the scattering vector. For the experiments we used bulk magnetite cleaved *in situ* and 40-nm thick magnetite films epitaxially grown by molecular-beam epitaxy on epipolished MgO (001) substrates, which were miscut by 6° towards [001] in order to create a stepped surface.

Figure 1(a) shows the RSXD spectra of the $(00\frac{1}{2})_c$ superstructure peak at Fe $L_{2,3}$ resonances for several azimuthal angles taken at 83 K from a thin film sample. The resonant spectra were recorded by varying the photon energy and keeping the momentum transfer constant [30]. Here, the azimuthal angle ϕ is defined to be zero when the wave vectors of the incoming and outgoing light are perpendicular to the step edges of MgO substrate and have positive components of descending direction of steps. For $\phi = 0°$, 90°, 180°, 270°, two axes of the cubic room-temperature unit cell are parallel to the scattering plane. The data show a clear azimuth and polarization dependence. For a symmetry study, we analyze the azimuthal-angle and polarization dependence of the $(00\frac{1}{2})_c$ peak intensity integrated along the $[001]_c$ direction in reciprocal space at the L_3 resonance maximum. The result is presented as symbols in Fig. 1(b). We observe a low-symmetry azimuthal pattern, which is only characterized by a mirror symmetry across the 0°–180° azimuth, i.e., along the direction perpendicular to the step edges of the substrate. Corresponding data for bulk magnetite are presented as symbols in Fig. 1(c). They show a slightly distorted fourfold symmetry. We hence conclude that because of epitaxial strain induced by the stepped substrate [31,32], only two out of four possible domains form with their monoclinic a_m axis rotated by ±45° from the mirror plane spanned by the 0°–180° azimuth and the $[001]_c$ direction. As a cross-check we present in Fig. 1(d) a polar plot generated by symmetrizing the film data in Fig. 1(b) with respect to the 90°–270° plane, thereby simulating a fully twinned sample. A fourfold pattern with the σ signal much stronger than the π signal for $\phi = 0°$, 90°, 180°, 270° and barely any polarization dependence for $\phi = 45°$, 135°, 180°, 270° as it is also found for the bulk sample is recovered.

We now discuss the space-group symmetry of the electronic state in the low-temperature phase. Since nearly all the spectral weight of the RSXD spectra is concentrated around the sharp peak at ~708 eV as seen in Fig. 1(a), we use a model, in which intermediate states are replaced by a single level. The scattering amplitude of RSXD within the

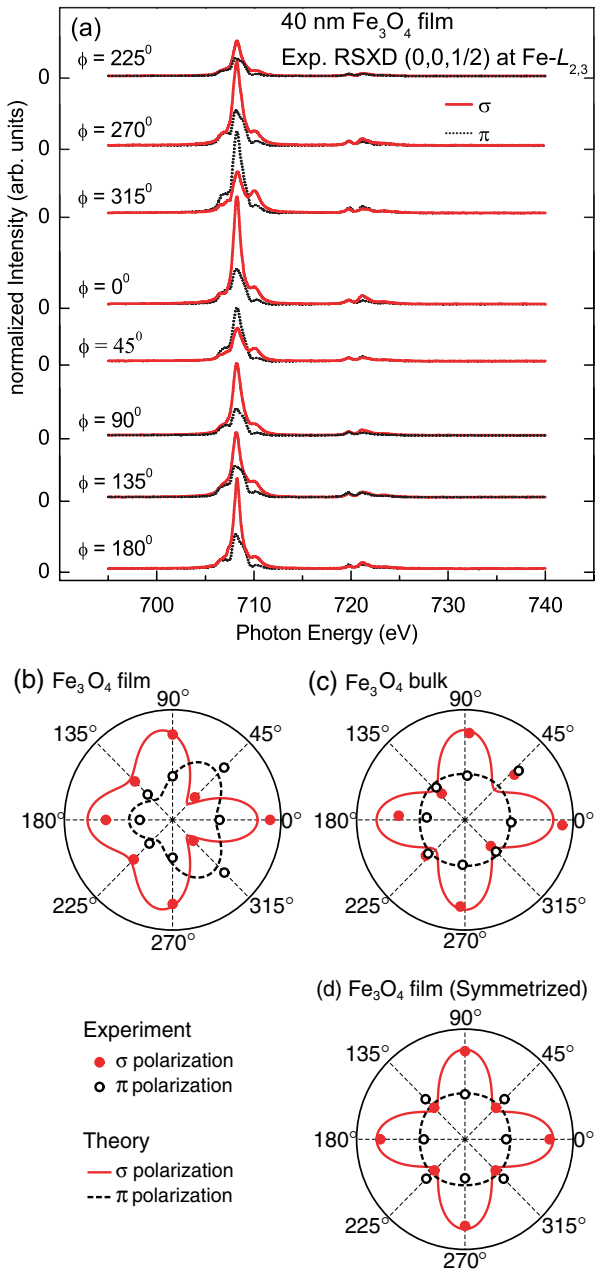

FIG. 1 (color online). (a) RSXD spectra of the $(00\frac{1}{2})_c$ peak at Fe $L_{2,3}$ resonances for σ (solid line) and π (dotted line) polarized light taken at 83 K from a Fe_3O_4 film grown on a stepped MgO substrate. (b) The azimuthal-dependent polar plot of the integrated $(00\frac{1}{2})_c$ peak intensity of L scan at Fe L_3 maximum taken from (a) (circles) compared with the single-level model calculations (lines); the closed (open) circles and the solid (dotted) lines correspond to those for σ (π) polarized light. (c) The same as (b) but for bulk sample. (d) The same as (b) but for symmetrized film data with respect to 90°–270° mirror plane to emulate fully twinned sample. For the calculations in (b), (c), and (d), the parameter set $\mathrm{Re}[F_{yz}]$:$\mathrm{Im}[F_{zx}]$:$\mathrm{Re}[F_{xy}] = 1$:0.63:0.63 is used. While two monoclinic domains with equal volumes restricted by epitaxial strain imposed by the stepped MgO substrate are assumed in (b), all of four possible monoclinic domains with equal volumes are considered in (c) and (d).

$2p \rightarrow 3d$ electric dipole transition at this resonant maximum can be written as

$$A(\boldsymbol{\varepsilon}, \boldsymbol{\varepsilon}') = i\sum_l \exp(i\boldsymbol{q}\cdot\boldsymbol{R}_l)\sum_{i,j}\varepsilon_i\varepsilon'_j f_{ij}^{(l)}, \quad (1)$$

where $f_{ij}^{(l)}$ represents the scattering tensor of site l at the position $\boldsymbol{R}_l$ and $\boldsymbol{\varepsilon}$ and $\boldsymbol{\varepsilon}'$ denote the polarization vectors of the incident and scattered light, respectively; $\boldsymbol{q}$ is the scattering vector. Here, we use the same definition of the coordination for the atomic positions on the $a_c/\sqrt{2} \times a_c/\sqrt{2} \times 2a_c$ pseudo-$Pmca$ cell as in Ref. [8]. There are six unique B sites labeled $B1a$, $B1b$, $B2a$, $B2b$, $B3$, and $B4$. Unlike at the Fe or O K-edge resonances, the scattering intensities at the Fe $L_{2,3}$ edge are sensitive to the direction of spin moment of the excited site because of large spin-orbit interaction of the $2p$ core hole in the intermediate state [33]. Therefore, the transformation of the magnetic moments on each Fe site by the symmetry operations should also be taken into account. For the magnetization direction along the c_m axis (which is the easy axis [34]) and the $Pmca$ lattice structure, the symmetry of the low-temperature phase including the magnetic order is $P\underline{mc}a$.

Although the lattice structure of the low-temperature phase of Fe_3O_4 is well described by the pseudo-orthorhombic $Pmca$ with a slight monoclinic $P2/c$ distortion, this does not imply that the deviation toward the monoclinic symmetry is necessarily also small in the electronic state. In general, the symmetry of the system having the magnetization direction perpendicular to the b_m axis is lowered to $P\underline{2}/\underline{c}$: the σ_a mirror plane is removed whereas symmetry operations $\{\Theta\sigma_b|\frac{c_m}{2}\}$ and $\{\Theta C_2|\frac{c_m}{2}\}$ are retained, where Θ denotes the time-reversal operator. The scattering amplitude of the $(00\frac{1}{2})_c$ reflection caused by the Fe ions on the B sites can be written as

$$A(\boldsymbol{\varepsilon}, \boldsymbol{\varepsilon}') \propto (\varepsilon_y\varepsilon'_z + \varepsilon_z\varepsilon'_y)\mathrm{Re}[F_{yz}] + i(\varepsilon_z\varepsilon'_x - \varepsilon_x\varepsilon'_z)\mathrm{Im}[F_{zx}] + (\varepsilon_x\varepsilon'_y + \varepsilon_y\varepsilon'_x)\mathrm{Re}[F_{xy}], \quad (2)$$

with

$$F_{ij} = 2(f_{ij}^{(1a)} + f_{ij}^{(1b)}) + 4\cos 2\pi z_3 f_{ij}^{(3)} + 4\cos 2\pi z_4 f_{ij}^{(4)},$$

where $z_3 \sim 3/8$ and $z_4 \sim 3/8$ are the z coordinates of the $B3$ and $B4$ sites, respectively, and there is no contribution from the $B2a$ and $B2b$ sites. Note that if the $P\underline{mc}a$ symmetry is assumed, i.e., without monoclinic distortion, the term with $\mathrm{Re}[F_{xy}]$ would vanish. The scattered intensities with σ-polarized ($\mu = \sigma$) and π-polarized ($\mu = \pi$) incident light are

$$I_\mu(\phi_m) = |A(\boldsymbol{\varepsilon}_\mu, \boldsymbol{\varepsilon}'_\sigma)|^2 + |A(\boldsymbol{\varepsilon}_\mu, \boldsymbol{\varepsilon}'_\pi)|^2, \quad (3)$$

where

$$\boldsymbol{\varepsilon}_\sigma = \boldsymbol{\varepsilon}'_\sigma = (-\sin\phi_m, \cos\phi_m, 0)$$
$$\boldsymbol{\varepsilon}_\pi = (\cos\phi_m \sin\theta, \sin\phi_m \sin\theta, \cos\theta)$$
$$\boldsymbol{\varepsilon}'_\pi = (-\cos\phi_m \sin\theta, -\sin\phi_m \sin\theta, \cos\theta) \quad (4)$$

and $\theta \approx 31.3°$ represents the Bragg angle; ϕ_m denotes the azimuth angle for a single domain and is $\phi_m = 0$ when the scattering plane is parallel to the x axis (a_m axis). Within this single intermediate-state approximation, the azimuth and polarization dependence of the intensity of the $(00\frac{1}{2})_c$ reflection can be parametrized by only three components of the scattering matrices $\mathrm{Re}[F_{yz}]$, $\mathrm{Im}[F_{zx}]$, and $\mathrm{Re}[F_{xy}]$.

To compare the results with the experiments, in Fig. 2 reflection intensities as the functions of the azimuthal angle with three different parameter sets are drawn with the solid (σ polarization) and dashed (π polarization) lines. On the top row of Fig. 2, those for the single-domain crystal $I_\mu(\phi_m)$ are shown; on the bottom row, those for a twinned crystal as a model for the Fe_3O_4 layer on the stepped MgO surface are depicted, where crystal domains rotated by $\pm 45°$ around the z axis are assumed to coexist with the same volume, i.e., $\bar{I}_\mu(\phi) \equiv \frac{1}{2}[I_\mu(\phi + 45°) + I_\mu(\phi - 45°)]$. While the shapes of the intensity curves in (a) and (b) corresponding to $P\underline{mc}a$ are centrosymmetric, those for $P\underline{2}/\underline{c}$ in (c) are noncentrosymmetric. More clear differences in the shapes between the intensity curves for the $P\underline{mc}a$ and $P\underline{2}/\underline{c}$ symmetries are found in those for the twinned crystal presented on the bottom in the figure. Unlike the experimental observation, those for $P\underline{mc}a$ have no angular dependence. In contrast, the intensities for $P\underline{2}/\underline{c}$ have a prominent polarization and angular dependence and agree well with the experimental intensities in Fig. 1(b) (the calculations with the optimal choice of the

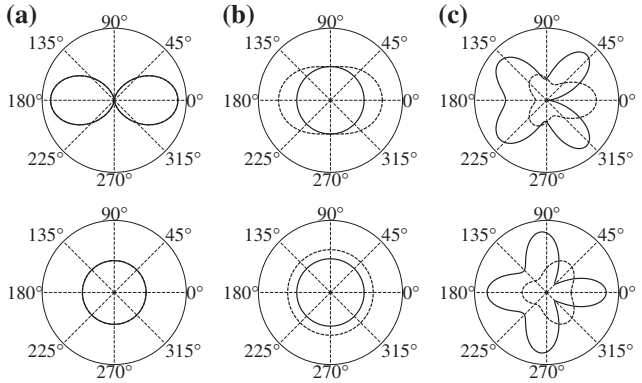

FIG. 2. Azimuth and polarization dependence of the $(00\frac{1}{2})_c$ reflection intensities. The solid and dashed lines denote the intensities with the σ- and π-polarization light, respectively. Those for the single-domain crystal (top row) and for the Fe_3O_4 layer on the stepped MgO substrate (bottom row) are depicted. The choices of the three components of the scattering matrices in (a) and (b) are for $P\underline{mc}a$, and those in (c) are for $P\underline{2}/\underline{c}$; their ratios for $\mathrm{Re}[F_{yz}]$:$\mathrm{Im}[F_{zx}]$:$\mathrm{Re}[F_{xy}]$ are (a) 1:0:0; (b) 1:1:0; and (c) 1:1:1.

parameter set $\mathrm{Re}[F_{yz}]$:$\mathrm{Im}[F_{zx}]$:$\mathrm{Re}[F_{xy}] = 1{:}0.63{:}0.63$ are presented as lines in this figure). Also, the bulk data are reproduced with the same parameter set if four domains with equal volumes are considered [lines in Fig. 1(c)].

To obtain the experimentally observed degree of noncentrosymmetric shape in Fig. 1(b), the value of $\mathrm{Re}[F_{xy}]$ must be comparable to that of $\mathrm{Re}[F_{yz}]$. This indicates that the observed deviation from the orthorhombic $Pmca$ symmetry below T_V is not at all small. Since the value of $\mathrm{Re}[F_{xy}]$ relative to $\mathrm{Re}[F_{yz}]$ due to the small monoclinic lattice distortions should be on the order of $|\cos\beta| \approx 0.004$ [24], the large value of $\mathrm{Re}[F_{xy}]/\mathrm{Re}[F_{yz}] \sim 0.6$ shows that the symmetry of the $3d$ electronic state is remarkably lowered toward monoclinic $P2/c$. Note that here, the analysis is limited to the $a_c/\sqrt{2} \times a_c/\sqrt{2} \times 2a_c$ subcell but there still remains the possibility that the symmetry is lowered further to a monoclinic symmetry group with the $\sqrt{2}a_c \times \sqrt{2}a_c \times 2a_c$ cell such as $C2/c$ or Cc.

The observation of a prominent azimuth and polarization dependence, which is the hallmark of the monoclinic symmetry, also for the bulk sample verifies that the lower Fe $3d$ electronic symmetry in respect to lattice symmetry is not due to a particular film sample but is an intrinsic property of magnetite.

Our finding of $\mathrm{Re}[F_{xy}]/\mathrm{Re}[F_{yz}] \sim 0.6$ directly excludes that the $(00\frac{1}{2})_c$ superstructure simply reflects lattice distortions as claimed in Refs. [23–25], which would result in a ratio on the order of 0.004. Contrary to the common lattice knowledge of magnetite below T_V, we find that the space-group symmetry of $3d$ wave function has much lower symmetry being truly monoclinic $P2/c$ or even lower. As the $(00\frac{1}{2})_c$ superstructure peak is a glide-plane forbidden reflection, the diagonal elements of the scattering tensor do not contribute. The presence of this peak, hence, cannot originate directly from a charge order. Of course one would consider that charge order as postulated in Refs. [7,8] can be observed indirectly through orbital polarization due to the lattice distortion induced by the charge order. However, this orbital polarization, then, should follow the pseudo-$Pmca$ symmetry of the lattice. Thus, the only reasonable explanation is that what is observed at the $(00\frac{1}{2})_c$ peak is an orbital order (or a simultaneous orbital and charge order) with a true monoclinic symmetry, which is the primary order parameter of the Verwey transition, and that this prominent symmetry lowering of the electronic system is only slightly reflected in the lattice structure. This interpretation of an orbital order being the driven force of the Verwey transition is consistent with the fact that no clear sign of the symmetry lowering has been found in phonon dispersion measurements [35].

While our findings clearly prove the existence of orbital order in magnetite, they also impose constraints on what kind of orbital order this could be. Whatever the orbital and/or charge order in the $3d$ electronic state below T_V is, its symmetry cannot be *pseudo*-orthorhombic but must show a large deviation towards monoclinic. Band-structure studies succeeded in predicting the t_{2g}-orbital order in magnetite [16–19]. However, the resulting ROO-CO state obtained assuming the pseudo-$Pmca$ lattice has approximate $Pmca$ symmetry and deviations toward monoclinic are negligible (details of ordered orbitals in this ROO-CO state can be found in Table I in Ref. [18]). Therefore, this ROO-CO state cannot explain the large deviation toward monoclinic $P2/c$ symmetry found experimentally for the $(00\frac{1}{2})_c$ reflection. On the other hand, the COO state in Ref. [20] has true monoclinic $P2/c$ symmetry. This COO state spontaneously breaks the orthorhombic symmetry even when the monoclinic distortion of the pseudo-$Pmca$ lattice is omitted ($\beta = 90°$). In this orbital order, the occupied orbital on the $B1a$ site is essentially different from that on the $B1b$ site and orbitals on the $B3$ and $B4$ sites have no σ_a mirror symmetry. This COO model could hence be compatible with our experimentally found symmetry for orbital order in magnetite.

In summary, the azimuth-angle dependence of the $(00\frac{1}{2})_c$ reflection intensities is found to be affected more strongly by the space-group symmetry of the $3d$ state in the initial state than by that of the lattice. The symmetry of the $3d$ state is much more monoclinic than what would be expected from the pseudo-orthorhombic $Pmca$ lattice structure and is at least lowered to $P2/c$ magnetic space group. All this leads to the conclusion that the origin of the $(00\frac{1}{2})_c$ superstructure in Fe $L_{2,3}$ RSXD is orbital order. Most importantly, the revealed symmetry of the $3d$ state wave function and the fact that the symmetry is extremely deviated from that of the lattice impose strong restriction on possible orbital and charge ordering below T_V and candidates of the mechanism of the Verwey transition.

We thank Lucie Hamdan and the mechanical workshop of the II. Physikalische Institut for their skillful technical assistance. This work was supported by the Deutsche Forschungsgemeinschaft through SFB 608 and by the BMBF through Contracts No. 05KS7PK1, No. 05K10PK2, and No. 05ES3XBA/5.

[1] E. J. W. Verwey, Nature (London) **144**, 327 (1939).
[2] For review, see F. Walz, J. Phys. Condens. Matter **14**, R285 (2002); J. García and G. Subías, J. Phys. Condens. Matter **16**, R145 (2004).
[3] M. Iizumi and G. Shirane, Solid State Commun. **17**, 433 (1975).
[4] L. V. Gasparov, D. B. Tanner, D. B. Romero, H. Berger, G. Margaritondo, and L. Forró, Phys. Rev. B **62**, 7939 (2000).
[5] Y. Miyamoto and S. Chikazumi, J. Phys. Soc. Jpn. **57**, 2040 (1988).
[6] C. Medrano, M. Schlenker, J. Baruchel, J. Espeso, and Y. Miyamoto, Phys. Rev. B **59**, 1185 (1999).
[7] J. P. Wright, J. P. Attfield, and P. G. Radaelli, Phys. Rev. Lett. **87**, 266401 (2001).

[8] J. P. Wright, J. P. Attfield, and P. G. Radaelli, Phys. Rev. B **66**, 214422 (2002).
[9] For instance, see Y. Joly, J. E. Lorenzo, E. Nazarenko, J.-L. Hodeau, D. Mannix, and C. Marin, Phys. Rev. B **78**, 134110 (2008); J. Blasco, J. García, and G. Subías, Phys. Rev. B **83**, 104105 (2011).
[10] E. J. W. Verwey, P. W. Haayman, and F. C. Romeijn, J. Chem. Phys. **15**, 181 (1947).
[11] J. R. Cullen and E. R. Callen, Phys. Rev. B **7**, 397 (1973).
[12] Y. Yamada, Philos. Mag. B **42**, 377 (1980).
[13] M. Mizoguchi, J. Phys. Soc. Jpn. **70**, 2333 (2001).
[14] S. K. Mishra, Z. Zhang, and S. Satpathy, J. Appl. Phys. **76**, 6700 (1994).
[15] H. Seo, M. Ogata, and H. Fukuyama, Phys. Rev. B **65**, 085107 (2002).
[16] H.-T. Jeng, G. Y. Guo, and D. J. Huang, Phys. Rev. Lett. **93**, 156403 (2004).
[17] I. Leonov, A. N. Yaresko, V. N. Antonov, M. A. Korotin, and V. I. Anisimov, Phys. Rev. Lett. **93**, 146404 (2004).
[18] I. Leonov, A. N. Yaresko, V. N. Antonov, and V. I. Anisimov, Phys. Rev. B **74**, 165117 (2006).
[19] H.-T. Jeng, G. Y. Guo, and D. J. Huang, Phys. Rev. B **74**, 195115 (2006).
[20] H. Uzu and A. Tanaka, J. Phys. Soc. Jpn. **77**, 074711 (2008).
[21] D. J. Huang, H.-J. Lin, J. Okamoto, K. S. Chao, H.-T. Jeng, G. Y. Guo, C.-H. Hsu, C.-M. Huang, D. C. Ling, W. B. Wu, C. S. Yang, and C. T. Chen, Phys. Rev. Lett. **96**, 096401 (2006).
[22] J. Schlappa, C. Schüßler-Langeheine, C. F. Chang, H. Ott, A. Tanaka, Z. Hu, M. W. Haverkort, E. Schierle, E. Weschke, G. Kaindl, and L. H. Tjeng, Phys. Rev. Lett. **100**, 026406 (2008).
[23] S. B. Wilkins, S. Di Matteo, T. A. W. Beale, Y. Joly, C. Mazzoli, P. D. Hatton, P. Bencok, F. Yakhou, and V. A. M. Brabers, Phys. Rev. B **79**, 201102(R) (2009).
[24] S. R. Bland, B. Detlefs, S. B. Wilkins, T. A. W. Beale, C. Mazzoli, Y. Joly, P. D. Hatton, J. E. Lorenzo, and V. A. M. Brabers, J. Phys. Condens. Matter **21**, 485601 (2009).
[25] S. Di Matteo, J. Phys. Conf. Ser. **190**, 012008 (2009).
[26] C. W. M. Castleton and M. Altarelli, Phys. Rev. B **62**, 1033 (2000).
[27] K. J. Thomas, J. P. Hill, S. Grenier, Y-J. Kim, P. Abbamonte, L. Venema, A. Rusydi, Y. Tomioka, Y. Tokura, D. F. McMorrow, G. Sawatzky, and M. van Veenendaal, Phys. Rev. Lett. **92**, 237204 (2004).
[28] S. S. Dhesi, A. Mirone, C. De Nadaï, P. Ohresser, P. Bencok, N. B. Brookes, P. Reutler, A. Revcolevschi, A. Tagliaferri, O. Toulemonde, and G. van der Laan, Phys. Rev. Lett. **92**, 056403 (2004).
[29] C. Schüßler-Langeheine, J. Schlappa, A. Tanaka, Z. Hu, C. F. Chang, E. Schierle, M. Benomar, H. Ott, E. Weschke, G. Kaindl, O. Friedt, G. A. Sawatzky, H.-J. Lin, C. T. Chen, M. Braden, and L. H. Tjeng, Phys. Rev. Lett. **95**, 156402 (2005).
[30] C. F. Chang, J. Schlappa, M. Buchholz, A. Tanaka, E. Schierle, D. Schmitz, H. Ott, R. Sutarto, T. Willers, P. Metcalf, L. H. Tjeng, and C. Schüßler-Langeheine, Phys. Rev. B **83**, 073105 (2011).
[31] J. Brötz, H. Fuess, T. Haage, and J. Zegenhagen, Phys. Rev. B **57**, 3679 (1998).
[32] J. Brötz and H. Fuess, in *Studies of High Temperature Superconductors*, edited by A. Narlikar (Nova Science Publishers, New York, 2002), Vol. 41, pp. 129–146.
[33] S. W. Lovesey, E. Balcar, K. S. Kinght, and J. Fernández Rodríguez, Phys. Rep. **411**, 233 (2005).
[34] K. Abe, Y. Miyamoto, and S. Chikazumi, J. Phys. Soc. Jpn. **41**, 1894 (1976).
[35] E. J. Samuelsen and O. Steinsvoll, Phys. Status Solidi B **61**, 615 (1974).